Open-Loop Distributed Beamforming Using Wireless Phase and Frequency Synchronization

Serge R. Mghabghab, *Graduate Student Member, IEEE*, Sean M. Ellison, *Member, IEEE* and Jeffrey A. Nanzer, *Senior Member, IEEE*

***Abstract*—Coordinating the operations of separate wireless systems at the wavelength level can lead to significant improvements in wireless capabilities. We address a fundamental challenge in distributed radio frequency system cooperation — inter-node phase alignment — that must be accomplished wirelessly, and is particularly challenging when the nodes are in relative motion. We present a solution to this problem that is based on a novel technique combining high-accuracy ranging and frequency transfer. We demonstrate the system in the first fully-wireless open-loop coherent distributed beamforming experiment. Inter-node range estimation to support phase alignment was performed using a two-tone stepped frequency waveform with a single pulse, while a two-tone waveform was used for frequency synchronization. The approach was implemented on a two-node dynamic system using Ettus X310 software-defined radios, with coherent beamforming at 1.5 GHz.**

***Index Terms*—Antenna arrays, disaggregated antennas, distributed beamforming, frequency synchronization, ranging.**

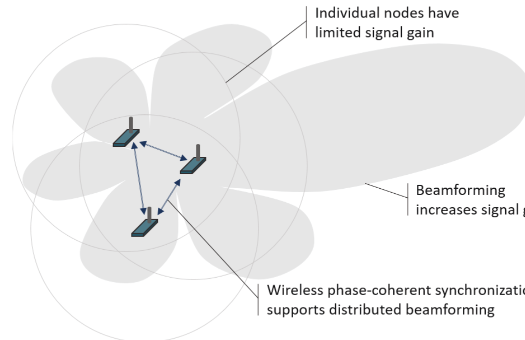

Fig. 1. Wireless phase-coherent coordination at the wavelength level supports distributed beamforming, increasing capabilities such as operational range over individual platform capabilities.

I. Introduction

Coordinating separate wireless systems at the wavelength level supports the ability to disaggregate wireless operations from a platform-centric model to a distributed network of coordinated devices, representing a paradigm shift in wireless system functionality. Without centralized system limitations, greater flexibility can be achieved in terms of scalability, adaptivity to changing conditions or requirements, and lower overall system costs as wireless performance parameters can be directly extended by adding low-cost elements to the network. Of the functions enabled by distributed wireless systems, distributed beamforming, where nodes coordinate to steer a phase-coherent wireless signal to a destination, is among the most significant (Fig. 1). However, along with these significant benefits come significant implementation challenges. The principal requirement for distributed beamforming is phase coherence among all nodes in the network, which must be accomplished wirelessly, at an accuracy within a fraction of the wavelength of the beamforming signal.

Manuscript received 2021.

This work was supported in part by the National Science Foundation (grant number 1751655), the Defense Advanced Research Projects Agency (grant number N66001-17-1-4045) and the Office of Naval Research (grant number N00014-17-1-2886). The views, opinions, and/or findings contained in this article are those of the author and should not be interpreted as representing the official views or policies, either expressed or implied, of the Defense Advanced Research Projects Agency or the Department of Defense.
(Corresponding Author: Jeffrey A. Nanzer)

S. R. Mghabghab and J. A. Nanzer are with the Department of Electrical and Computer Engineering, Michigan State University, East Lansing, MI 48824 USA (e-mail: mghabgha@msu.edu, nanzer@msu.edu).

S. M. Ellison was with the Department of Electrical and Computer Engineering, Michigan State University, East Lansing, MI 48824 USA. He is now with the Johns Hopkins University Applied Physics Laboratory, Laurel, MD 20723 USA (e-mail: elliso65@msu.edu).

Wavelength-level node synchronization has been approached using closed-loop architectures where the distributed nodes coordinate using feedback from the targeted location or from other external systems [1]–[5]. Such approaches simplify the node coordination process and make coherent beamforming possible as long as the network is operating in a cooperative environment. For applications such as radar and remote sensing, beamforming to locations without coherent feedback is necessary, and thus open-loop architectures, where no external feedback is needed, are required [6], [7]. Coordinating open-loop distributed wireless networks requires the nodes to synchronize in phase, frequency, and time to support and maintain beamforming. Such phase coherence necessitates high-accuracy ranging techniques to estimate the delays needed to correct for the relative phase shifts between the distributed nodes [1], [8]–[10]. Furthermore, maintaining phase coherence is not possible unless all the nodes are frequency locked [11]–[15]. Finally, time alignment is needed to ensure that pulses and symbols overlap; timing accuracy is thus dependent on the information rate [16]–[19].

In this paper, we demonstrate the first open-loop distributed beamforming at 1.5 GHz using fully wireless phase and frequency coordination in a dynamic distributed two-node system in relative motion. High-accuracy inter-node ranging for phase alignment is achieved using a spectrally sparse, scalable ranging waveform while frequency synchronization is supported by transmitting a two-tone modulated frequency reference which is demodulated using a self-mixing receiver. Whereas our prior work investigated inter-node range estimation and frequency synchronization independently [20], [21], this work is the first to demonstrate the feasibility of fully wireless open-loop distributed beamforming on mobilized platforms. We demonstrate a two-node distributed system based on software-defined radios (SDRs), transmitting 1.5 GHz continuous wave (CW) signals towards end-fire, which is the most challenging steering angle. Experimental results demonstrate the ability to maintain greater than 90% of the ideal beamforming power.

II. Inter-Node Range Estimation

Monitoring the positional change produced by the relative motion of the nodes within a coherent distributed system is essential to enable coherent beamforming, since any change in relative phase of the transmitted signals will impact the coherent summation of the signals. In a primary/secondary hierarchical architecture, every secondary node must track its position in comparison to a reference point, which is the location of the primary node. Based on a high-accuracy inter-node range measurement, the relative phase shifts can be calculated. The ranging waveform that is implemented shall be capable to support accurate delay estimation, unambiguous range determination, and scalability so it can be used by multiple nodes simultaneously to reduce the update latency.

The ranging two-tone stepped frequency waveform (TTSFW) that is used in this work is based on a spectrally sparse two-tone waveform, which has been proven to have optimal performance as a time delay estimator, in which the obtainable accuracy is dependent on the spectral separation of the tones [22]. The TTSFW uses a two-tone format on a pulse-by-pulse basis where the frequencies are monotonically increased with time and is expressed as [20]

$$s_t(t) = \frac{1}{\sqrt{N}} \sum_{n=0}^{N-1} \text{rect}\left(\frac{t-nT_r}{T}\right) \times \left(e^{j2\pi f_1 t} + e^{j2\pi f_2 t}\right) e^{j2\pi n \delta f t}, \quad (1)$$

where f_1 is the lower tone of the two-tones per pulse, f_2 is the upper tone, δf is the frequency step, N is the number of pulses, T_r is the pulse time duration, and T is the nonzero portion of the pulse duty cycle. The frequency step is given by $\delta f = \frac{BW}{2N-1}$ where BW is the total waveform bandwidth. The higher of the two frequencies is given by $f_2 = f_1 + \Delta f$ where $\Delta f = N\delta f$. The number of pulses in the TTSFW is dependent on the number of unique ranging connections made, where N pulses can be used to service $N!$ connections. A system consisting of two nodes, one primary and one secondary, has only one unique connection and therefore only a single pulse is need. The sampling frequency in this work was set to 25 MHz, the frequencies of TTSFW were selected as $f_1 = 500$ kHz and $f_2 = 4.5$ MHz, and the pulse repetition interval had a duration of 1 ms with a 50% duty cycle.

Matched filtering was used to estimate the delay. The processing gain from using a matched filter process is equivalent to the time-bandwidth product $N \cdot T \cdot BW_n$, where BW_n is the noise bandwidth. For the two-node system in this work, $N = 1$, $T = 0.5$ ms, $BW_n = 25$ MHz. The average pre-processing SNR was 30 dB, supported by a high-gain retransmission from the primary node, and the processing gain was equivalent to 41 dB giving a total post processing SNR of 71 dB. Using the Cramer-Rao lower bound [20], the timing variability can be solved for as $\sigma_\tau^2 = 9.885 \times 10^{-23}\ s^2$ and the lower bound for positional standard deviation can be found as $\sigma_x = 1.5$ mm.

III. Wireless Frequency Synchronization

Frequency synchronization was accomplished using an adjunct self-mixing analog circuit [14]. The system block diagram is shown in Fig. 2. The circuit demodulates a beat frequency from a two-tone CW signal and inputs the resultant frequency to a phase-locked loop (PLL) to lock the oscillator of the secondary node. In this work the oscillators of the secondary node used a 10 MHz reference frequency, thus the two-tone frequency separation of the waveform was 10 MHz. As demonstrated in [14], the output of the self-mixing circuit is expressed as

$$V_{\text{ref}}(t) = \cos\left[2\pi\left(f_{r2} - f_{r1}\right)t + \phi_3\right], \quad (2)$$

where $\phi_3 = \phi_2 - \phi_1$, ϕ_1 and ϕ_2 are the phases of the two tones that can be tracked from the change of the inter-node separation Δd_{IN} between the primary and secondary nodes. The change in the phase constant of the output, $\Delta\phi_{\text{ref}}$, can be determined by estimating the phase shifts for the two received frequencies $\Delta\phi_1$ and $\Delta\phi_2$,

$$\Delta\phi_1 = -\frac{f_{r1} \cdot \Delta d_{IN} \cdot 360^\circ}{c}, \quad (3)$$

$$\Delta\phi_2 = -\frac{f_{r2} \cdot \Delta d_{IN} \cdot 360^\circ}{c}, \quad (4)$$

$$\Delta\phi_{\text{ref}} = \Delta\phi_2 - \Delta\phi_1 = -\frac{f_{\text{ref}} \cdot \Delta d_{IN} \cdot 360^\circ}{c}, \quad (5)$$

where $f_{\text{ref}} = f_{r2} - f_{r1}$ is the frequency of the reference signal. $\Delta\phi_{\text{ref}}$ is negative when the separation between the two nodes increases because the received signal is delayed. Once the shift of the output phase is determined, the phase changes of the transmitted signal can be tracked. Signals generated from the SDR's internal oscillator retain phase information and therefore the effect of the phase changes of the oscillators on the transmitted carrier can be represented by

$$\Delta\phi_{c_1} = \frac{f_c}{f_{\text{ref}}}\Delta\phi_{\text{ref}}, \quad (6)$$

where f_c is the carrier frequency.

It is important to note that the phase $\Delta\phi_{\text{ref}}$ in (5) is only dependent on the tone separation f_{ref} and not the actual frequencies used to transmit the two-tones. As a result, the final phase shift reflected on the transmitted carrier $\Delta\phi_{c_1}$ will only depend on the transmitted carrier frequency f_c and not the synchronization frequencies f_{r2} and f_{r1}, as shown in (6).

The phase shift $\Delta\phi_{c_1}$ is generated by the displacement of the primary antenna transmitting the two-tone synchronization waveform to the receiver of the frequency locking circuit. However another phase shift, $\Delta\phi_{c_2}$, which is proportional to the displacement d_T of the antennas performing the beamforming, manifests on the secondary node as well, and is given by $\Delta\phi_{c_2} = -\frac{1}{\lambda_c}\Delta d_T \sin(\theta) \cdot 360^\circ$, where θ is the beam steering angle and λ_c is the wavelength of the beamforming frequency. Beamforming is possible in a dynamic array once $\Delta\phi_{c_1}$ and $\Delta\phi_{c_2}$ are accounted for.

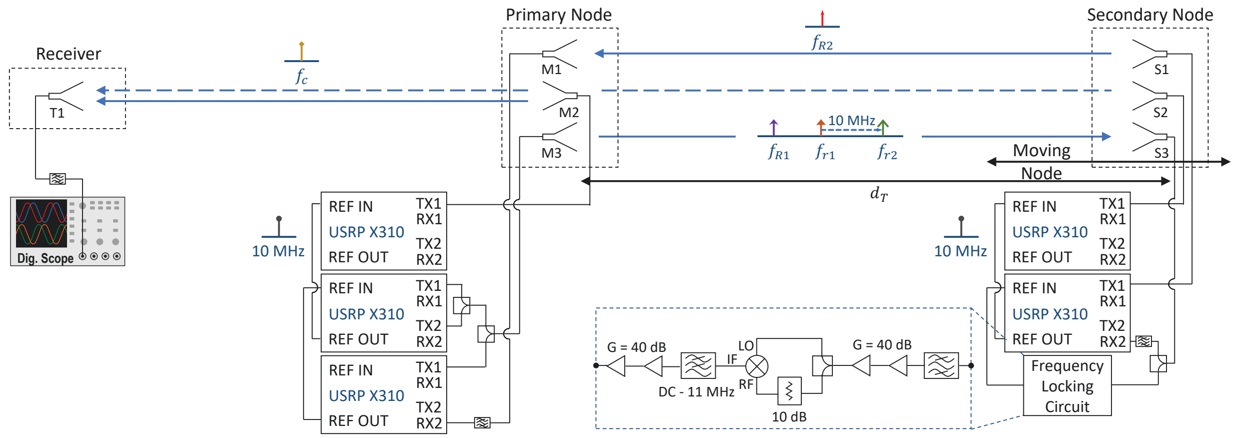

Fig. 2. Block diagram of the two-node open-loop distributed beamforming experiment.

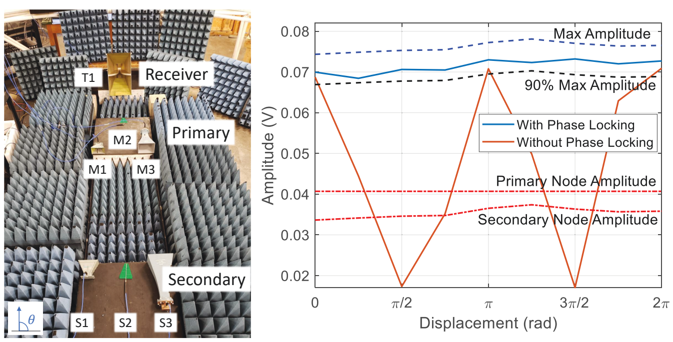

Fig. 3. (Left) Experimental setup of the open-loop coherent distributed array, set in a semi-enclosed antenna range. (Right) Beamforming results. The orange line shows the result of synchronizing the frequency but not the phase, while the blue line shows both frequency and phase synchronization.

IV. Distributed Beamforming Experiment

The block diagram along with an image of the experimental setup in a semi-enclosed arch range are shown in Figs. 2 and 3. The synchronization signals were transmitted using standard gain horn antennas where M1 and S1 had an operational frequency range of 2-18 GHz, while the antennas used for M3 and S3 had an operational frequency range of 3.95-5.85 GHz. Two log-periodic antennas with an operational frequency range of 1.35-9.5 GHz were used for the coherent beamforming antennas M2 and S2. The target receiver consisted of an oscilloscope connected to a horn antenna with operational frequency range of 0.5-6 GHz. The primary node was equipped with an active repeater that captured the ranging waveforms from the secondary node, amplified them, and retransmitted them back to the secondary node. By doing this, the propagation losses were proportional to $1/R^2$ rather than $1/R^4$ as seen in traditional radar, enabling higher received SNR and helping to mitigate the impact of any multipath signals. The carrier frequencies f_{R1} and f_{R2} of the transmit and receive channels of the repeater were separated far outside the instantaneous bandwidth of the receivers on the SDRs to minimize interference. The ranging waveform was transmitted from the secondary node using S1 at a carrier frequency of 3 GHz and retransmitted from M3 to S3 at a carrier frequency of 5 GHz. The frequency synchronization signals were also transmitted from the same horn antenna M3 where f_{r1} and f_{r2} were 4.3 GHz and 4.31 GHz respectively.

Based on the SNR of the received ranging waveform, the positional uncertainty is expected to be close to 1.5 mm. An analysis on ranging requirements for coherent beamforming in [21] indicates that an uncertainty of less than 6 mm is required for beamforming operations at 1.5 GHz with a steering angle $\theta = 90°$ (which has the most stringent phase alignment requirements), which was supported by the described ranging parameters. At the beginning of the test, the static phase offset ϕ_0 was calibrated; this calibration represents a one-time calibration performed when the system is powered on. The two transmitters were operated continuously and the secondary node was moved relative to the primary node in 2.5 cm increments over a total distance of λ_c (20 cm), yielding a total differential signal phase change of 720° from the change in inter-node range and the phase change due to the delay of the frequency synchronization signal.

The results of the wireless beamforming experiment are shown in Fig. 3 for multiple cases: transmitting from each node individually, transmitting from both nodes with only wireless frequency locking, and transmitting from both nodes with frequency locking and phase correction from the range estimation. The maximum possible signal amplitude and 90% of the maximum amplitude derived from the individual signal amplitudes are also shown. With only frequency locking, the received signal undergoes two cycles of constructive and destructive interference as expected. When the ranging system estimates the phase change and updates the transmitted signal phase, the received signal is above 90% throughout the experiment, demonstrating open-loop coherent distributed beamforming.

V. Conclusion

We demonstrated the first fully wireless open-loop phase-coherent distributed beamforming experiment with relative node displacement. Based on a joint high-accuracy ranging method and wireless frequency transfer, the approach is scalable to larger arrays, and can support general wireless operations including communications and sensing.

References

[1] Y.-S. Tu and G. J. Pottie, "Coherent cooperative transmission from multiple adjacent antennas to a distant stationary antenna through awgn channels," in *Vehicular Technology Conference. IEEE 55th Vehicular Technology Conference. VTC Spring 2002 (Cat. No. 02CH37367)*, vol. 1. IEEE, 2002, pp. 130–134.

[2] D. R. Brown III and H. V. Poor, "Time-slotted round-trip carrier synchronization for distributed beamforming," *IEEE Transactions on Signal Processing*, vol. 56, no. 11, pp. 5630–5643, 2008.

[3] R. Mudumbai, G. Barriac, and U. Madhow, "On the feasibility of distributed beamforming in wireless networks," *IEEE Transactions on Wireless communications*, vol. 6, no. 5, pp. 1754–1763, 2007.

[4] Z. Ding, W. H. Chin, and K. K. Leung, "Distributed beamforming and power allocation for cooperative networks," *IEEE Transactions on Wireless Communications*, vol. 7, no. 5, pp. 1817–1822, 2008.

[5] V. Havary-Nassab, S. Shahbazpanahi, and A. Grami, "Optimal distributed beamforming for two-way relay networks," *IEEE Transactions on Signal Processing*, vol. 58, no. 3, pp. 1238–1250, 2009.

[6] J. A. Nanzer, R. L. Schmid, T. M. Comberiate, and J. E. Hodkin, "Open-loop coherent distributed arrays," *IEEE Transactions on Microwave Theory and Techniques*, vol. 65, no. 5, pp. 1662–1672, 2017.

[7] R. L. Schmid, S. M. Ellison, T. M. Comberiate, J. E. Hodkin, and J. A. Nanzer, "Microwave wireless coordination technologies for coherent distributed maritime radar," in *2017 IEEE MTT-S International Microwave Symposium (IMS)*, June 2017, pp. 884–887.

[8] I. C. Sezgin, M. Dahlgren, T. Eriksson, M. Coldrey, C. Larsson, J. Gustavsson, and C. Fager, "A low-complexity distributed-mimo testbed based on high-speed sigma–delta-over-fiber," *IEEE Transactions on Microwave Theory and Techniques*, vol. 67, no. 7, pp. 2861–2872, 2019.

[9] F. Quitin, A. T. Irish, and U. Madhow, "A scalable architecture for distributed receive beamforming: Analysis and experimental demonstration," *IEEE Transactions on Wireless Communications*, vol. 15, no. 3, pp. 2039–2053, 2016.

[10] H. Pilaram, M. Kiamari, and B. H. Khalaj, "Distributed synchronization and beamforming in uplink relay asynchronous ofdma comp networks," *IEEE Transactions on Wireless Communications*, vol. 14, no. 6, pp. 3471–3480, 2015.

[11] I. L. Syllaios, P. T. Balsara, and R. B. Staszewski, "On the reconfigurability of all-digital phase-locked loops for software defined radios," in *2007 IEEE 18th International Symposium on Personal, Indoor and Mobile Radio Communications*. IEEE, 2007, pp. 1–6.

[12] W.-Q. Wang, "Carrier frequency synchronization in distributed wireless sensor networks," *IEEE Systems Journal*, vol. 9, no. 3, pp. 703–713, 2014.

[13] M. Hamouda, G. Guarin, M. Gardill, B. Läemmle, R. Weigel, D. Kissinger, and T. Ussmueller, "A clock synchronization for m-sequence-based ultra-wideband systems," *IEEE Transactions on Microwave Theory and Techniques*, vol. 62, no. 12, pp. 3549–3561, 2014.

[14] S. Mghabghab and J. A. Nanzer, "A self-mixing receiver for wireless frequency synchronization in coherent distributed arrays," in *2020 IEEE MTT-S International Microwave Symposium (IMS)*. IEEE, 2020.

[15] O. Abari, H. Rahul, D. Katabi, and M. Pant, "Airshare: Distributed coherent transmission made seamless," in *2015 IEEE Conference on Computer Communications (INFOCOM)*. IEEE, 2015, pp. 1742–1750.

[16] R. L. Schmid, T. M. Comberiate, J. E. Hodkin, and J. A. Nanzer, "A distributed rf transmitter using one-way wireless clock transfer," *IEEE Microwave and Wireless Components Letters*, vol. 27, no. 2, pp. 195–197, 2017.

[17] S. Traverso and J. Bernier, "Low complexity time synchronization based on digital predistortion coefficients," *IEEE Microwave and Wireless Components Letters*, vol. 29, no. 3, pp. 240–242, 2019.

[18] D. R. Brown and A. G. Klein, "Precise timestamp-free network synchronization," in *2013 47th Annual Conference on Information Sciences and Systems (CISS)*, 2013, pp. 1–6.

[19] M. Li, S. Gvozdenovic, A. Ryan, R. David, D. R. Brown, and A. G. Klein, "A real-time implementation of precise timestamp-free network synchronization," in *2015 49th Asilomar Conference on Signals, Systems and Computers*, 2015, pp. 1214–1218.

[20] S. M. Ellison and J. A. Nanzer, "High-accuracy multi-node ranging for coherent distributed antenna arrays," *IEEE Transactions on Aerospace and Electronic Systems*, pp. 1–1, 2020.

[21] S. R. Mghabghab and J. A. Nanzer, "Open-loop distributed beamforming using wireless frequency synchronization," *IEEE Transactions on Microwave Theory and Techniques*, vol. 69, no. 1, pp. 896–905, 2020.

[22] J. A. Nanzer and M. D. Sharp, "On the estimation of angle rate in radar," *IEEE Transactions on Antennas and Propagation*, vol. 65, no. 3, pp. 1339–1348, 2017.